MINERALOGY OF THE VALLES MARINERIS: INITIAL STRATIGRAPHIC RESULTS FROM COMPARING TES ENDMEMBER COMPOSITIONS WITH MOLA. F. S. Anderson[1], V.E. Hamilton[1], and P.R. Christensen[2], [1]University of Hawai'i at Manoa, Hawai'i Institute of Geophysics and Planetology, 1680 East-West Road, POST 526B, Honolulu, HI 96822 (anderson@higp.hawaii.edu), [2]Dept. Geological Sciences, ASU, Box 876305, Tempe, AZ 85287-6305, (phil.christensen@asu.edu).

Introduction: This study tests the proposition that data from the Mars Global Surveyor Thermal Emission Spectrometer (MGS TES) and Mars Orbiting Laser Altimeter (MOLA) can be used to identify stratigraphic and mineralogic layering in the wall and floor deposits of the Valles Marineris (VM). By using TES data at full resolution to identify unique local compositional signatures, our study complements previous studies that averaged data at a regional scale [1]. The absolute elevation, dip, and stratigraphic relationships of observed layering in wall rock is determined using MOLA data. The observed composition and stratigraphic relationships can then be used to constrain the formation process of the Valles Marineris.

Background: TES is currently acquiring thermal infrared (5 – 50 μm) spectra of the Martian surface at spatial resolutions of approximately 3 x 6 km per pixel [2]. Spectral absorptions in Martian mid-IR data are attributable to atmospheric CO_2 and dust, water-ice clouds, and surface materials. *Smith et al.* [3] and *Bandfield et al*. [5-6] have demonstrated that the spectral signatures of the atmospheric components may be removed via radiative transfer modeling, and to first order, by linear deconvolution. The surface spectrum that remains after atmospheric removal is indicative of several properties of the surface materials including bulk composition, relative abundances of minerals, and particle size. The easiest surface spectra to interpret are those obtained in low-albedo, high thermal inertia regions that are dominated by coarse (10's – 100's of μm) sands, regolith, and/or bedrock with little dust. Using visible imaging, the Valles Marineris have been characterized as having significant layered deposits, a wide variety of morphologies, and numerous regions with low albedo surfaces.

It is important to note that the slopes of the canyon walls in the VM can be steep (up to 34°) causing TES to observe sloped surfaces. Slopes may become a problem in regions where steeply dipping walls meet near-horizontal surfaces (e.g., at the bottom of a canyon wall), which could create spectral complications due to the complex interaction of the radiated energy from the two surfaces [*P. Christensen*, personal communication, 2000]. Hence, in addition to constraining the stratigraphy and mineralogy of the VM, the results of this study will contribute to understanding this effect. The MOLA data used for this study were derived from the 128 pixel/degree digital elevation model. TES data points were collocated with MOLA data gridded to TES resolution.

Method: First we made compositional maps of the end member deconvolutions of the TES dataset that are performed with each downlink from MGS. These maps were then plotted on images of the topography of the

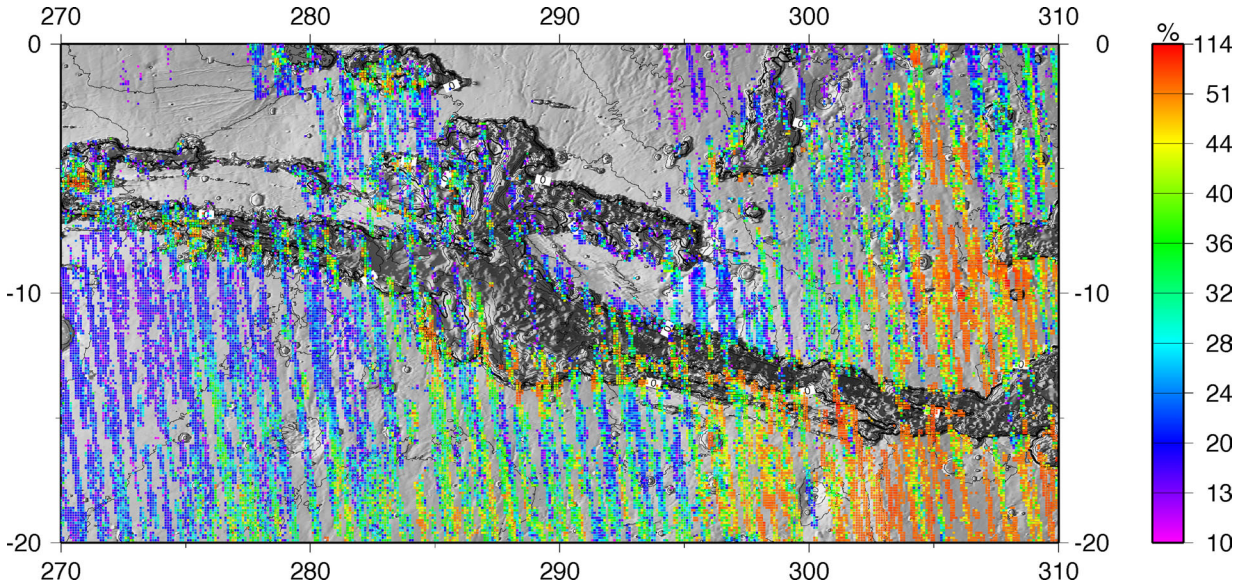

Figure 1: TES data for Basalt end member, over MOLA shaded relief with 1 km contour. Only concentrations exceeding the ~10% detection limit [7] and [4] are plotted. Note that the lower elevations of the eastern VM are highly basaltic, as are the southern walls and central troughs in Coprates, Melas, Ius, Noctis, potions of Candor, and Hebes Chasma. Regions with high albedo are left blank.

VM (e.g. Fig. 1). The predicted end members are based on the deconvolution method of *Smith et al.* [3] and *Bandfield et al.* [4] that atmospherically correct all incoming TES spectra using seven atmospheric and surface end members (two dust, two water-ice cloud, basalt, basaltic andesite, and hematite). As these end members are derived from the observed data, they are not "ideal" end members, and may in fact have shallower absorptions than some surface locales; hence they can be present at concentrations slightly higher than 100% of the surface. Furthermore, these areas are not representative of every possible surface, and may map some regions with only moderate success [*J. L. Bandfield*, pers. comm., 2003].

The TES data were constrained by avoiding bad orbit flags, orbits beyond 7000 (after which spacecraft vibration influenced the spectra), data with temperatures < 260K, or albedo > 0.24. The data were further decimated by removing end member estimates >120% (caused by processing errors) or with spectral RMS misfits > 0.015 (to provide tight constraints on results; median misfit in the VM data is 0.05).

The abundance of water ice and/or dust in the atmosphere can adversely influence the estimate of surface mineralogy. Unfortunately, the variance of atmospheric components as a function of season indicated that dust storms at ~L_s 240 influence much of the data. To minimize masking of the surface, we further constrained the data by requiring dust concentrations to be < 0.15.

Our second technique plotted TES end member mineralogy as a function of MOLA topography, slopes < 2°, and slopes > 2°. These plots indicate the relative abundance of end member mineralogies as a function of elevation for canyon walls and the surrounding plateaus, and can potentially identify stratigraphic layers.

Results: A histogram of net end member abundance as a function of L_s indicated that the basaltic andesite, dust, and ice components changed as a function of season. Dust and ice, as previously reported, demonstrate an inverse correlation, while the basaltic andesite end member is influenced by overlap with a band with a dust band [*J. L. Bandfield*, pers. comm., 2003]. Thus, this study focuses on the basaltic and hematite end members, as they are stable with L_s.

The map of basalt displays two levels of end member concentration; one generally >30%, the other generally <24%. The higher concentration is topographically lower, and may extend from the basin of Solis Dorsa northwards under a region of low basalt concentration until it crops out in the wall of the VM. These materials may also represent aeolian draping, or a mineralogic change with no stratigraphic relationship. The high concentration of basalt is also spatially associated with the Hesperian ridged plains (*Hr*), Noachian subdued craters (Npl_2), and ridged units (*Nplr*) [6], and

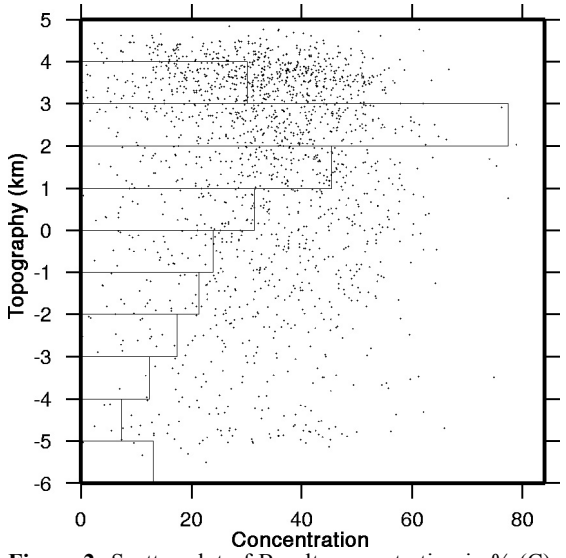

Figure 2: Scatter plot of Basalt concentration in % (C) and topography (T) for Coprates Chasma. Histogram shows topography associated with C-T points. Only points associated with the walls of VM (slopes >2°) are shown. Note the increased number of points between 4-5 km, which given it's relative lack of topographic abundance, represents a strong surface concentration.

may be consistent with low viscosity volcanism identified for *Hr*. Lastly, the superposed younger plains of Syria, Solis, and Sinai are associated with andesitic compositions. Our observations of hematite in the Valles Marineris are similar to those seen by *Christensen et al.*, [7].

Figure 2 is an example of the 2nd approach showing the elevation of basalt concentrations for slopes >2°, primarily constraining the results to the walls of VM. These graphs were made for regional and local areas in Coprates, Melas, Ius, Hebes, and Candor. These maps generally indicate the presence of a basaltic layer at a mean elevation of 4-5 km, and a second, less concentrated layer from –2 to -1 km.

Conclusion: Our initial results suggest that TES can resolve a vertically stratified layer increasing in age with depth. These initial results represent the first steps in correlating the layering and mineralogy of the VM. The complete analysis will focus on local multi-component deconvolution as regions of interest are identified in the 7 end member data.

References: [1] Bandfield et al., *Science*, *287*, 1626-1630, 2000. [2] Christensen et al., *J. Geophys. Res.*, *97*, 7719-7734, 1992. [3] Smith et al., *J. Geophys. Res.*, *105*, 9589-9607, 2000. [4] Bandfield et al., *J. Geophys. Res.*, *105*, 9573-9587, 2000. [5] Scott and Tanaka, USGS, Geologic map of Mars, *M 15M 0/90 G*, Flagstaff, Ariz.,1986. [6] Christensen et al., *J. Geophys. Res.*, 2002. [7] *Christensen et al., J. Geophys. Res.*, *105*, 9609-9621, [2000a].